The chemodynamical memory of a major merger in a NIHAO-UHD⋆ Milky Way analogue II: Were Splash stars heated or already born hot?

Sven Buder,[1]†‡ Tobias Buck,[2,3] Ása Skúladóttir,[4] Melissa Ness,[1] Madeleine McKenzie,[5]§ and Stephanie Monty[6,7]

[1]*Research School of Astronomy and Astrophysics, Australian National University, Canberra, ACT 2611, Australia*
[2]*Universität Heidelberg, Interdisziplinäres Zentrum für Wissenschaftliches Rechnen, Im Neuenheimer Feld 205, D-69120 Heidelberg, Germany*
[3]*Universität Heidelberg, Zentrum für Astronomie, Institut für Theoretische Astrophysik, Albert-Ueberle-Straße 2, D-69120 Heidelberg, Germany*
[4]*Dipartimento di Fisica e Astronomia, Universitá degli Studi di Firenze, Via G. Sansone 1, I-50019 Sesto Fiorentino, Italy*
[5]*The Observatories of the Carnegie Institution for Science, 813 Santa Barbara Street, Pasadena, 91101, CA, USA*
[6]*Institute of Astronomy, University of Cambridge, Madingley Road, Cambridge CB3 0HA, UK*
[7]*Department of Astronomy, New Mexico State University, Las Cruces, NM 88003, USA*

Accepted 2025 Month DD. Received 2025 Month DD; in original form 2025 October 15

ABSTRACT

One of the most debated consequences of the Milky Way's last major merger is the so-called *Splash*: stars with disc-like chemistry but halo-like kinematics, often interpreted as evidence for the violent heating of an early protodisc. Using the same high-resolution NIHAO-UHD cosmological simulation analysed in Buder et al. (2025b, hereafter Paper I), we test whether a Splash-like population arises naturally in a Milky Way analogue. By tracing stellar birth positions, ages, and present-day orbits, we find no evidence for widespread dynamical *splashing* of in-situ stars. Instead, protodisc stars were already born on dynamically hot orbits, with the transition to a rotation-supported disc occurring only during or after the merger. The observed Splash may therefore reflect the turbulent early disc, subsequently intermixed with accreted stars and those formed from merger-driven gas inflows, rather than a distinct merger-heated population. Our results suggest an alternative to the proposed splashing, and highlight the need to disentangle the relative contributions of merger-induced heating and intrinsically hot disc formation in order to clarify the nature of Splash-like stars and their role in shaping the early Milky Way.

Key words: Galaxy: evolution – Galaxy: formation – Galaxy: structure – Galaxy: abundances – Galaxy: kinematics and dynamics

1 INTRODUCTION

A long-standing goal of Galactic archaeology is to reconstruct how mergers shaped the early Milky Way. Thanks to *Gaia* astrometry (Brown 2021) and large spectroscopic surveys (Jofré et al. 2019), it is now clear that our Galaxy experienced at least one major accretion event about 8–10 Gyr ago, commonly referred to as the *GSE* merger (Haywood et al. 2018; Belokurov et al. 2018; Helmi et al. 2018; Naidu et al. 2020). This event left an imprint in the stellar halo, and growing evidence suggests that it also influenced a pre-existing disc, dynamically mixing the earliest in-situ populations with accreted debris (Helmi 2020).

One of the most debated signatures of this process is the so-called Splash population (Belokurov et al. 2020; Belokurov & Kravtsov 2022). These stars appear chemically similar to the old, α-enhanced thick disc, but occupy hotter, halo-like orbits. Their dual nature has made them central to arguments about whether the *GSE* merger violently heated the protodisc, or whether some old stars were already born on dynamically hot orbits in our Galaxy's turbulent youth.

Observational studies first pointed to an in-situ halo component overlapping with the disc in chemistry. Bonaca et al. (2017) identified metal-rich, prograde halo stars consistent with a heated thick disc origin. Expanding on this, Bonaca et al. (2020) used *Gaia* DR2 and H3 survey data to argue that disc-like chemistry but halo-like kinematics reflect merger-driven heating, providing a timeline for disc perturbation shortly after *GSE*. Similarly, Di Matteo et al. (2019, 2020) interpreted metal-rich, eccentric stars as evidence that the *GSE* merger dynamically heated pre-existing disc stars into the halo, strengthening the case that Splash stars trace this violent epoch.

Other studies have argued for alternative or complementary origins. In a hydrodynamical simulation of an isolated clumpy disc, Amarante et al. (2020) showed that a Splash-like component can form without mergers: stars scattered by giant clumps during early, turbulent disc phases naturally occupy low-angular-momentum, halo-like orbits, yet remain chemically continuous with the thick disc. More recently, cosmological simulations have broadened the picture. Dillamore et al. (2022) found that Splash-like stars could be a generic feature of Milky Way analogues, while Dillamore et al. (2023) showed that bar resonances can also create halo-like substructures. Extending this, Dillamore & Sanders (2025) demonstrated that secular evolution can reshape integral-of-motion space, complicat-

⋆ NIHAO-UHD is the Ultra High Definition re-run of a Milky Way analogue from the *Numerical Investigation of a Hundred Astronomical Objects* (NIHAO) suite (Wang et al. 2015).
† E-mail: sven.buder@anu.edu.au
‡ Australian Research Council DECRA Fellow
§ NASA Hubble Fellow

ing attempts to uniquely attribute Splash stars to merger heating. Observationally, Kisku et al. (2025) showed that Splash stars occupy the high-α, high-[Al,K/Fe], low-[Mn/Fe] extension of the thick disc sequence, and, in combination with ARTEMIS simulations (Font et al. 2020), argued that both major and minor mergers can produce Splash-like signatures, in agreement with the conclusions from the HESTIA simulation by Khoperskov et al. (2023b).

Taken together, these studies highlight that Splash stars remain a crucial but unresolved tracer of the Milky Way's formative history. They may represent violently heated disc stars, stars born hot in a turbulent proto-disc, or a mixture of both, possibly reshaped by subsequent secular evolution. The distinction matters: if Splash stars are heated, they provide a dynamical clock for the last major merger; if they are born hot, they instead reflect the conditions of the early disc, independent of mergers.

In Buder et al. (2025b, hereafter Paper I), we used a NIHAO-UHD cosmological simulation of a Milky Way analogue (Buck 2020; Buck et al. 2021) to examine the chemodynamical memory of a major merger. Paper I focused on the efficiency of recovering accreted stars in integral-of-motion space, the preservation of their birth radii, and chemical evolution. Building on this framework, this work (Paper II) asks whether a Splash-like population emerges in a fully cosmological Milky Way analogue, and if so, whether these stars were *heated by the merger or already born hot*. Our guiding questions are:

(i) Does a distinct Splash population emerge in a high-resolution cosmological simulation?
(ii) Is this population born in the Milky Way analogue or also/only the *GSE*-like galaxy that merged with it around 8.6 Gyr ago?
(iii) Are Splash-like stars dynamically heated, or do they form already hot in the turbulent early disc?
(iv) What does the simulated Splash imply for interpreting the Milky Way's merger-driven history?

2 SIMULATION DATA

We use the same high-resolution cosmological zoom-in simulation analysed in Paper I, namely the NIHAO-UHD Milky Way analogue `g8.26e11` (Wang et al. 2015; Buck et al. 2019, 2020, 2021). The simulation was performed with the smoothed-particle hydrodynamics code `Gasoline2` (Wadsley et al. 2017), following the NIHAO feedback and enrichment framework (Stinson et al. 2006, 2013; Wang et al. 2015). It adopts a ΛCDM cosmology as inferred by Planck Collaboration et al. (2014) and includes metal-line cooling, star formation, and stellar feedback with chemical enrichment from asymptotic giant branch stars, core-collapse supernovae, and supernovae of type Ia (Buck et al. 2021). The NIHAO-UHD suite reaches ultra-high mass resolution; for `g8.26e11` the stellar particle mass is $7.5 \times 10^3\,M_\odot$.

This simulation was chosen because it closely resembles the Milky Way in its global properties, such as stellar mass and disc-dominated morphology, and experienced a last major merger at a lookback time of $\sim$ 8.6 Gyr, broadly consistent with the timing inferred for the Milky Way's *GSE* merger (Helmi et al. 2018; Naidu et al. 2021). At $z = 0$, the main halo has a virial radius of $R_{200} = 206$ kpc and a total mass of $M_{200} = 9.1 \times 10^{11}\,M_\odot$, including $8.2 \times 10^{11}\,M_\odot$ in dark matter, $6.4 \times 10^{10}\,M_\odot$ in gas, and $2.3 \times 10^{10}\,M_\odot$ in stars. The last major merger progenitor, a *GSE*-like galaxy, had a stellar mass of $\sim 3 \times 10^9\,M_\odot$ and a total mass ratio of roughly 1 : 5 relative to the host at the time of infall, comparable to empirical estimates for the Milky Way's *GSE* merger (e.g. Helmi et al. 2018; Naidu et al. 2021). A key structural property of `g8.26e11` is that it forms a multi-armed spiral disc but no significant present-day bar (Buder et al. 2025a). This means that bar-driven resonances, proposed as a possible driver of the *Splash* by Dillamore et al. (2022, 2023), are likely not responsible for the features we analyse here.

A full description of the simulation setup, feedback and enrichment prescriptions, and comparison to Milky Way constraints is given in Sec. 2.1 of Paper I. Sec. 2.2 of Paper I details how we trace the birth positions of stars in discrete 100 Myr time steps relative to the evolving centre of mass of the main halo. Combined with the orbital energies and actions (Sec. 2.3 of Paper I), which we computed with the AGAMA code (Vasiliev 2019), this enables us to distinguish in-situ stars from those accreted during mergers, as described in Sec. 3.1 of Paper I.

3 ANALYSIS: THE MERGER PROCESS AND ITS CHEMODYNAMICAL EFFECTS

In Paper I, we analysed the NIHAO-UHD Milky Way analogue to classify stars into in-situ and accreted populations, examine their orbital properties and selection efficiency in integrals-of-motion space, and evaluate how well birth positions and chemical evolution are retained as chemodynamical memory. Building on this framework, we now focus on the merger's dynamical effects. Our aim is to assess whether the simulation produces a population analogous to the observationally claimed Splash: stars born in the early disc but dynamically heated onto halo-like orbits, stars formed from merger-driven gas mixing, or stars that may be misclassified accreted populations. By linking these possibilities back to the classification, dynamical, and chemical analyses of Paper I, we investigate whether the Splash emerges as a distinct component or as the overlap of several processes.

3.1 Infall

In Fig. 3 of Paper I we studied the birth positions of accreted stars within their host galaxy in timesteps of 0.1 Gyr. The birth positions in the $X_{\rm birth}$ vs. $Z_{\rm birth}$ plane (Fig. 3b of Paper I) demonstrated that the major merger galaxy followed an almost diagonal merger path. When tracking the orbits of the accreted stars born within 50 kpc of the main galaxy, we calculate the inclination angle θ of the merger (with larger inclination meaning a more edge-on rather than face-on trajectory) to be between 34 and 55 deg, based on a singular value decomposition in three dimensions or a linear fit in $X_{\rm birth}$ vs. $Z_{\rm birth}$, respectively. This value is roughly comparable to the inclination of $\theta = 30$ deg inferred by Naidu et al. (2021) for the Milky Way's *GSE* merger with simulations with multiple inclination and circularity values. We note that the pattern of stars on significantly more prograde orbits (Fig. 4b of Paper I) matches less well with the patterns of typically low absolute angular momenta observed in the Milky Way and simulated for a merger with circularity $\eta = 0.5$. Our orbit pattern rather matches the simulation outcome by Naidu et al. (2021) for a highly circular galaxy with $\eta = 0.9$ (see their Fig. 3). We refrain from interpreting this, however, as there are more particular merger parameters that might play an important role for energy and momentum transfer. This includes the path along which the merging galaxy spiralled into the larger galaxy relative to the galactic plane (see $X_{\rm birth}$ vs. $Y_{\rm birth}$ in Fig. 3a of Paper I), as well as the locations of passages through this plane. We can, however, study the kinematic/dynamical effect on already born in-situ stars as well as the chemodynamic effect on stars that formed during the merger.

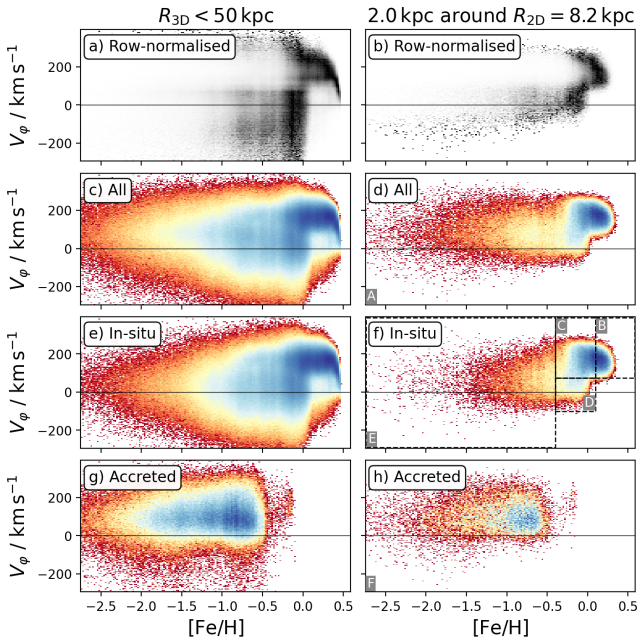

Figure 1. Iron abundance [Fe/H] vs. azimuthal velocity V_φ for stars within $R_{3D} < 50$ kpc (left panels) and the Solar-like locus (right panels). Panels a) and b) show the density distribution, when normalising the density across each row, as done by Belokurov et al. (2020, see their Fig 1). Panels c) and d) show the logarithmic density distribution of all stars. Panels e) and f) show in-situ stars, while panels g) and h) show accreted stars. Dashed black rectangles with letters A-F at their lower left corner annotate the selection of different subsamples of the Solar neighbourhood.

3.2 Selection of Splash-like stars

Based on a population of stars in the Solar neighbourhood that are more metal-rich than typical halo stars yet follow highly eccentric orbits, Belokurov et al. (2020) proposed that these stars originated in the Milky Way's disc and were *splashed* onto low-angular-momentum orbits during the last major merger. Motivated by this hypothesis, we analyse stars in our Milky Way analogue in the same plane as Belokurov et al. (2020), namely [Fe/H] vs. azimuthal velocity V_φ, both for the entire galaxy and for a Solar neighbourhood-like region (see Fig. 1).

In a first step, we replicate the density distribution plots in [Fe/H] vs. V_φ space that Belokurov et al. (2020, their Fig. 1) used to identify Splash stars. We show both the row-normalised density distribution in Figs. 1a and 1b as well as the logarithmic density distributions in Figs. 1c and 1d. Here we indeed find a strikingly similar distribution in [Fe/H] vs. V_φ space to that observed by Belokurov et al. (2020) for the Solar neighbourhood. In particular, we recover the sickle-like distribution of highest densities (black) around [Fe/H] ~ -0.25 in the row-normalised distribution of Fig. 1b, which Belokurov et al. (2020) attributed to the three zones of thin disc (top), thick disc (middle), and Splash (bottom).

In the other panels of Fig. 1 with logarithmic density distributions, metal-poor in-situ stars exhibit a broad spread in azimuthal velocity, up to $\pm 300\,\mathrm{km\,s^{-1}}$) centred around $V_\varphi = 0\,\mathrm{km\,s^{-1}}$. Both Yu et al. (2023b) and Chandra et al. (2024) described this as the first of three phases of disc evolution, the chaotic bursty phase. As metallicity increases, the stellar density rises and peaks around $-0.4 <$ [Fe/H] < 0.1 for stars with $V_\varphi < 0\,\mathrm{km\,s^{-1}}$. In this metallicity range, we observe a steep increase in the average V_φ. This the second phase of disc evolution (Chandra et al. 2024) is also described as spin-up/bursty-disc phase (Yu et al. 2023b). Finally, the most metal-rich stars are moving on rotationally supported disc orbits with a narrower distribution of $200 \pm 100\,\mathrm{km\,s^{-1}}$ (the third, thin-disc phase of disc evolution in Yu et al. 2023b; Chandra et al. 2024).

In observations, the interpretation of the [Fe/H]-V_φ plane is complicated by uncertainties in stellar ages and the unknown birth locations of stars. In contrast, our simulation allows us to overcome these limitations by providing both precise stellar ages and a clear distinction between in-situ and accreted stars. Taking advantage of this, we define several subsamples of the Solar neighbourhood (Sample A, Fig. 1d) to probe the nature of the Splash population. Sample D (Fig. 1f) selects in-situ Splash-like stars with $-0.4 <$ [Fe/H] < 0.1 and $-100 < V_\varphi < 75\,\mathrm{km\,s^{-1}}$. More generally, we then define:

- Sample A: all stars in the Solar neighbourhood (Fig. 1d) and from within this region we sub-select (Figs. 1f and 1h):
- Sample B: more metal-rich in-situ stars ([Fe/H] > 0.1),
- Sample C: in-situ stars with Splash-like [Fe/H] but higher V_φ,
- Sample D: the Splash stars themselves,
- Sample E: more metal-poor in-situ stars ([Fe/H] < -0.4), and
- Sample F: accreted stars in the Solar neighbourhood.

While we identify the Splash-like sample D in Fig. 1 at $-0.4 <$ [Fe/H] < 0.1 in the simulation, we note that Belokurov et al. (2020) found it as slightly lower metallicities of $-0.7 <$ [Fe/H] < -0.25 in the Milky Way's Solar neighbourhood. Because of the findings by Buck et al. (2021), who studied the influence of chemical evolution model choices, such as nucleosynthetic yields, on chemical evolution predictions on NIHAO-UHD simulations, we attribute this absolute offset in [Fe/H] and other abundances mainly to the choices of chemical evolution parameters in the simulation. Because of these abundance offsets, our selection is consistent with the *relative* position of Splash stars in the [Fe/H] vs. V_φ diagrams used by Belokurov et al. (2020), but not identical.

We also note that Belokurov et al. (2020) did not specifically select in-situ stars for their Splash sample. In the Milky Way analogue, however, we only find stars fitting the Splash selection criteria to be born in-situ (compare Figs. 1f and 1h in the Splash region). We find the accreted stars of the Milky Way analogue moving with higher azimuthal velocities of $V_\varphi = 100^{+80}_{-70}\,\mathrm{km\,s^{-1}}$ within the Solar neighbourhood (Fig. 1h), as compared to values of $V_\varphi = 20^{+100}_{-70}\,\mathrm{km\,s^{-1}}$ for *GSE* stars within the Milky Way's Solar neighbourhood (Buder et al. 2022).

3.3 Ages and chemistry of Splash-like stars

Before we take a look at possible changes to the dynamics and spatial distribution of these stars, we get an idea of their typical ages and chemistry in Figs. 2 and 3, respectively. In both spaces, we find the Splash stars as part of the in-situ sequence. This sequence extends from the oldest ($11.3^{+0.9}_{-0.7}$ Gyr) and most metal- and [Al/Fe]-poor in-situ stars to younger Splash stars ($9.2^{+0.7}_{-0.7}$ Gyr) with higher [Al/Fe]. From there, the sequence continues to even younger stars ($7.2^{+1.3}_{-3.8}$ Gyr), which have similar [Fe/H] but higher V_φ and [Al/Fe] and lower [Mg/Mn]. Finally, it reaches the youngest and most metal-rich in-situ stars ($3.8^{+2.0}_{-2.5}$ Gyr). Furthermore, we note that the accreted stars with ages of $11.2^{+1.3}_{-1.7}$ Gyr are for the most part older or at least as old as the Splash stars. This finding (of F older than D older than C) is consistent with the observations by Belokurov et al. (2020). In particular, we also find that the Splash-like stars are exclusively old,

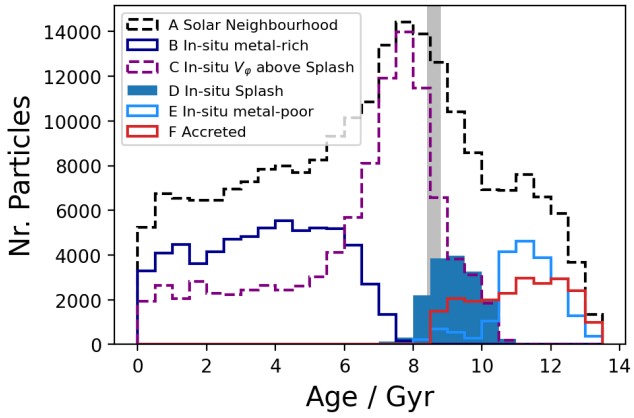

Figure 2. Age distribution of different samples of stars in the Solar neighbourhood as selected in the [Fe/H] vs. V_φ plane of Fig. 1. A grey bar indicates the time of the major merger around 8.6 Gyr.

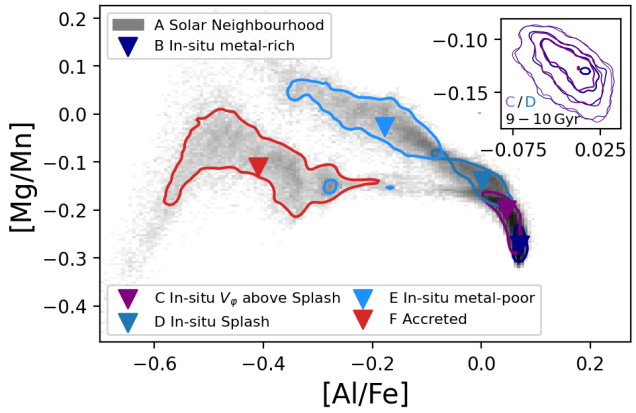

Figure 3. Abundance distribution in [Al/Fe] vs. [Mg/Mn] of different samples of stars in the Solar neighbourhood as selected in the [Fe/H] vs. V_φ plane of Fig. 1. Contours correspond to the 68 % highest-density interval. An inset figure is showing the distribution of samples C and D with ages of 9 – 11 Gyr, with contours showing the 40, 60, and 80 % highest-density intervals.

corroborating that they indeed could come from a Splash-like event. We also note that while there are stars with chemical compositions literally bridging the accreted (blue) and in-situ (red) populations, this bridge[1] connects at the low [Mg/Mn]-end of the Splash star region. As already noted by Buder et al. (2024), these stars (less than 1 % within the Solar neighbourhood) are likely formed from mixed gas during the merger, but do not contribute significantly (less than 9 %) to any of the sub-samples of the simulation's Solar neighbourhood.

More strikingly, we note only a little overlap in the distribution of ages and chemistry of the most metal-poor in-situ stars with the Splash stars within the Solar neighbourhood. The age distribution of the Splash stars (Sample D) is consistent with the oldest stars of the in-situ population with similar [Fe/H] but higher V_φ than the Splash stars (Sample C) and shows a similar profile especially for ages of 9 – 11 Gyr.

This result opens up a number of questions that evolve around how special the Splash stars are – both in terms of their chemistry as well as their orbits. While Belokurov et al. (2020) favoured a scenario in which the stars have been splashed by a major merger, they also discussed a scenario in which the stars might have been born dynamically hotter with more eccentric orbits. One could for example imagine these stars being the low azimuthal velocity tail of a dynamically hotter early disc. We thus take a closer look at the sample of stars with similar iron abundance ($-0.4 < [\mathrm{Fe/H}] < 0.1$) and the aforementioned ages of 9 – 11 Gyr.

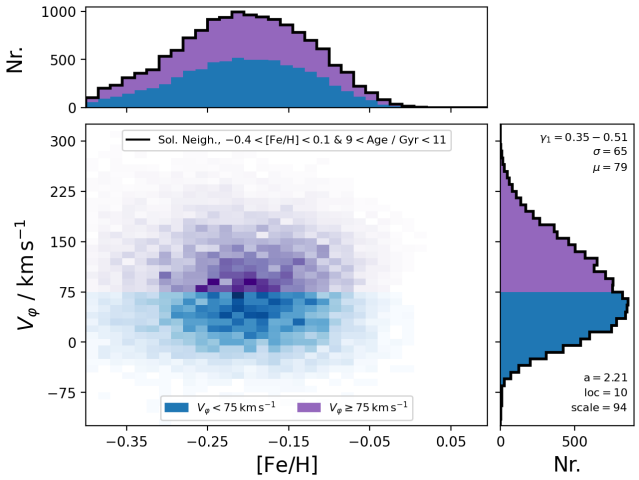

Figure 4. Distributions of [Fe/H] and V_φ for stars in the Solar neighbourhood at $-0.4 < [\mathrm{Fe/H}] < 0.1$. We show the stacked distribution (black lines) as well as 2-dimensional and 1-dimensional histograms of each distribution.

3.4 Coeval counterparts of Splash-like stars

In particular, we are interested in a comparison of properties of the low azimuthal velocity (Splash) stars with $V_\varphi < 75$ km s^{-1} and their higher azimuthal velocity counterpart. We show their distribution in a [Fe/H] vs. V_φ diagram in Fig. 4 and notice that their distribution both in 2-dimensions as well as each individual dimension appear rather smooth. In particular the distribution in V_φ appears normal-distributed with a slight positive skewness. We have thus used the SKEWNORM functionality of the SCIPY.STATS module (Virtanen et al. 2020) to fit a skewed normal distribution to the data, finding a distribution around 79 ± 65 km s^{-1} with a positive skewness of γ_1 between 0.35 and 0.51 when using SKEW or SKEWNORM, respectively. In addition, we have also looked into the chemical enrichment of the low- and high-V_φ samples, in particular [Al/Fe] and [Mg/Mn]. The samples are visually congruent with each other (see inset of Fig. 3) and distributed in the region of Fig. 3 of sample D. To statistically assess whether the two 2-dimensional distributions are drawn from the same underlying population, we apply the Maximum Mean Discrepancy test (Gretton et al. 2012) using the HYPPO package's KSAMPLE.MMD (Panda et al. 2019). The resulting test statistic of 10^{-6} with a p-value of 0.26 indicates no significant difference between the two samples. For reference, Kolmogorov–Smirnov tests (Hodges 1958) applied independently to the 1D marginals via SCIPY.STATS.KS_2SAMP also yield high p-values of 1.0 and 0.86. This leads to the conclusion that both the high V_φ and low V_φ Splash stars are drawn (born?) from the same distribution with a large spread in V_φ.

[1] The region of $-0.2 < [\mathrm{Al/Fe}] < -0.05$ and $[\mathrm{Mg/Mn}] < -0.14$.

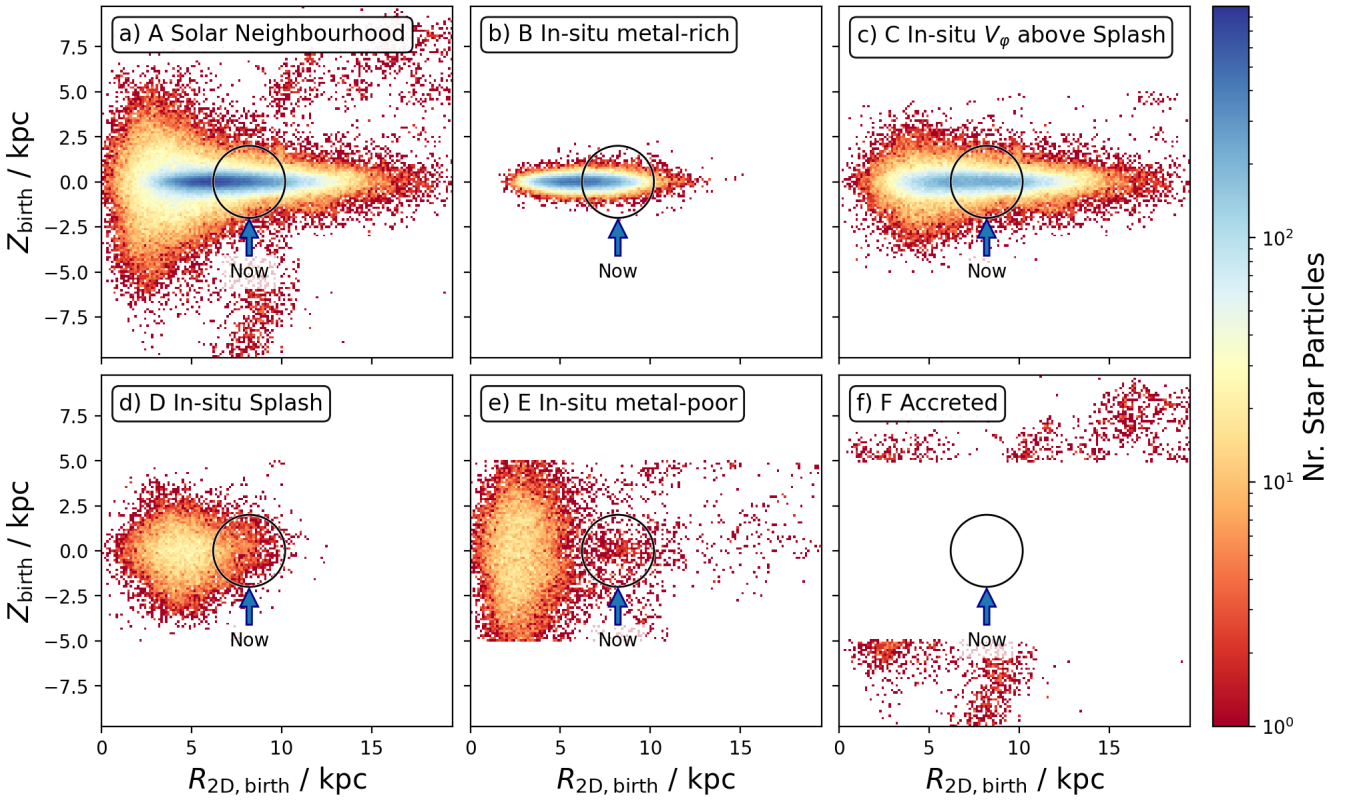

Figure 5. Density distribution of birth positions in galactocentric cylindrical coordinates $R_{\rm birth,2D}$ and $Z_{\rm birth}$ for star particles of samples A-F (corresponding to panels a-f) that are currently in the Solar neighbourhood (black circles) of 2 kpc around $R_{\rm 2D} = 8.2$ kpc. In panels e) and f) we note the imprint of our selection of in-situ vs. accreted stars via $|Z_{\rm birth}| > 5$ kpc (Eqs. 4 and 5 of Paper I).

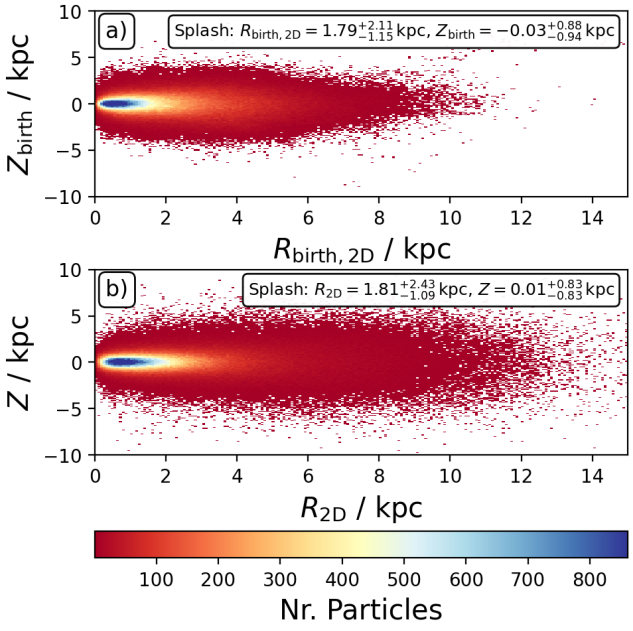

Figure 6. Radial and vertical distribution of Splash stars. Panel a) shows birth radii $R_{\rm birth,2D}$ and birth heights $Z_{\rm birth}$, whereas panel b) shows current radii $R_{\rm 2D}$ and heights Z. Text insets show the median and 16th to 84th percentiles of each distribution.

3.5 Birth and present-day orbits of Splash-like stars

To further establish, where – and by proxy on which orbits – the Splash stars were born, we analyse their and the other samples' birth positions in Fig. 5. The simulation makes remarkable predictions about the origin of stars that are currently residing in a small Solar neighbourhood-like region, with stars visiting from the centre of the galaxy or its furthest outskirts at 20 kpc (see Fig. 5a) – not to mention the accreted stars born even further away (Fig. 5f). In agreement with radial migration models (for example Frankel et al. 2018, 2020), a significant amount of metal-rich stars (Fig. 5b) is visiting from the inner galaxy (Sample B with 5-95th percentiles of $R_{\rm birth,2D} \sim 3.9-8.9$ kpc centred around a median of 6.3 kpc), while high-V_φ stars with Solar-like iron abundances (Sample C) show a larger distribution of birth origins along the disc ($R_{\rm birth,2D} \sim 3.5 - 12.5$ kpc, centred around 7.4 kpc). However, both the in-situ Splash ($R_{\rm birth,2D} \sim 2.2 - 7.8$ kpc, centred around 4.6 kpc) and the in-situ metal-poor stars ($R_{\rm birth,2D} \sim 1.0 - 9.7$ kpc, centred around 2.9 kpc) are basically born exclusively in the inner galaxy ($R_{\rm birth,2D} \ll 8.2$ kpc) and with a larger spread of $Z_{\rm birth}$, that is, not on a thinner disc.

Since the Splash stars were born further inwards, the question arises, whether they were born on more radially eccentric orbits which reach into our Solar neighbourhood, or if their orbits have significantly changed through the radial splashing that shifts their initially inner orbits to overlap with our Solar neighbourhood. Because our snapshot at redshift $z = 0$ only includes the present-day velocities, we turn to a comparison of birth and present-day spatial distribution in Fig. 6 in an effort to quantify the change of spatial

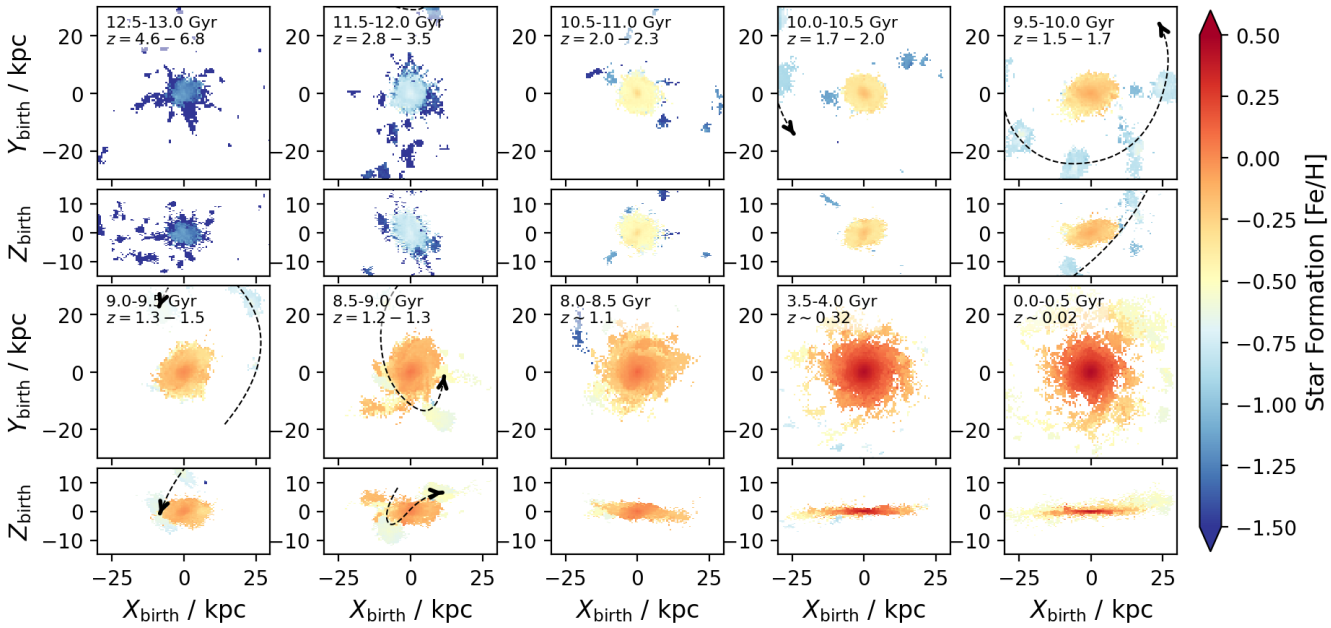

Figure 7. Distributions of iron abundances [Fe/H] for the face-on ($X_{\rm birth}$ vs. $Y_{\rm birth}$, odd rows) and edge-on ($X_{\rm birth}$ vs. $Z_{\rm birth}$, even rows) views in ten selected birth epochs within 0.5 Gyr, starting from 12.5 – 13.0 Gyr in the top-left panel to 0.0 – 0.5 Gyr in the bottom-right panel. Dashed black arrows indicate the path of the last major merger. See for figures with all epochs as well as colouring by density.

distributions which would imply a change of orbits. When comparing the birth (upper panel) with present-day (lower panel) density distributions in linear density, we note a more extended low-density envelope to higher radii. Similarly, we note an extend of larger Z-coverage for $R_{\rm 2D} > 6$ kpc – again with very low densities. The overall distribution of stars has, however, changed insignificantly. This is evident in the only minor change of the average $R_{\rm birth,2D} = 1.79^{+2.11}_{-1.15}$ kpc to $R_{\rm 2D} = 1.81^{+2.43}_{-1.09}$ kpc and $Z_{\rm birth} = -0.03^{+0.88}_{-0.94}$ kpc to $Z = 0.01^{+0.83}_{-0.83}$ kpc. When calculating the average of the change for the individual stars, we find $\overline{\Delta R_{\rm 2D}} = \overline{R_{\rm 2D,birth} - R_{\rm 2D}} = -0.1^{+1.1}_{-1.2}$ kpc and $\overline{\Delta|Z|} = \overline{|Z_{\rm birth}| - |Z|} = 0.03^{+0.70}_{-0.68}$ kpc. In our particular Milky Way analogue simulation, this thus implies little orbit change of these stars, or no significant splashing, with a possible exception of stars beyond $R_{\rm 2D} > 3.9$ kpc, the outermost 16 % of Splash stars (the 84th percentile of $R_{\rm birth,2D}$). We discuss the implications of this finding in Section 4.

3.6 Effect on newly forming stars

Although the main focus of our study is understanding the is to understand the properties and origin of the Splash, we want to briefly investigate the potential of the available birth positions to study the evolution of the main galaxy's density and chemical enrichment during and after the merging. For this purpose, we investigate the change of iron abundance [Fe/H] in birth positions in both the $X_{\rm birth}$ vs. $Y_{\rm birth}$ and $X_{\rm birth}$ vs. $Z_{\rm birth}$ dimensions in Fig. 7, with each panel showing the median iron abundance in each bin for stars formed within a selection of 10 star formation epochs that each span 0.5 Gyr. We remind ourselves that because birth positions are estimated in 0.1 Gyr steps, we expect the footprint of the major accretion to mimic up to five smaller galaxies, which in fact are showing the position of the same smaller galaxy in 0.1 Gyr steps (see especially the panels around 9.5 – 10.0 Gyr in these figures).

From these figures we can assess that the stars of the early main galaxy were born on typically random orbits leading to a spheroidal galaxy shape and new stars following similar orbits until a lookback time of ~ 10 Gyr. Between ~ 10 and ~ 8.5 Gyr ago, we then see the birth positions follow a more and more disc-like structure with increasing radii and decreasing heights. For ages below 8 Gyr, we then see star formation occurring within a rotationally supported disc. These observations are in agreement with the modelling by Minchev et al. (2013). Albeit qualitatively in agreement with the description of the *spin-up* by Belokurov & Kravtsov (2022), we would place the tracers of the spin-up phase exactly at the position of the Splash in the [Fe/H] vs. V_φ, not only more metal-poor than the Splash as done by Belokurov & Kravtsov (2022, see their Fig. 5b). A detailed assessment of how the smaller galaxy's gravitational influence and angular momentum transfer between ~ 10 and ~ 8.6 Gyr contributed to the spin-up of the Milky Way analogue's disc requires tracing gas and dark matter in addition to stars, which we leave to future work.

What we can investigate, however, is the change of star formation [Fe/H] during this time. This property is used as colour-coding for the different star formation epochs in Fig. 7. Here we see that after the initial main galaxy started forming stars with [Fe/H] ≤ −1.5 (dark blue), its core quickly started forming more metal-rich stars with the star formation [Fe/H] in the core rising from −1.0 to −0.75 between ~ 12.5 and ~ 11.5 Gyr ago, while several smaller amounts of metal-poor stars ([Fe/H] ≤ −1.5) where born outside of the core galaxy and quickly accreted. This process continues with star formation in the core reaching [Fe/H] ~ −0.2 and the outskirts reaching −0.35 at a lookback time of ~ 10 Gyr. At this time, we notice the arrival of the major merger galaxy to within 30 kpc distance. Its path is indicated with dashed arrows as it continues to form stars in each 0.1 Gyr snapshot and finally merge with the main galaxy in a spiral pattern around 8.6 Gyr ago. For this galaxy, we also note a negative metallicity gradient from core to outskirts, but at lower

metallicities than the main galaxy, in particular in the top-right panel of Fig. 7. Such gradients were also found by other simulation studies (Amarante et al. 2022; Khoperskov et al. 2023a; Mori et al. 2024; Carrillo et al. 2025). Most importantly, we notice that while the metallicity of the major merger galaxy tends to still increase and reach [Fe/H] ~ -0.5 until ~ 8.5 Gyr ago, the main galaxy's star formation [Fe/H] seems to not decrease within the inner $R_{\rm birth,2D} < 10$ kpc (compare the snapshots of $8.5 - 9.0$ Gyr with $8.0 - 8.5$ Gyr for that region). Only in the outskirts of the galaxy at $10 \lesssim R_{\rm birth,2D} \lesssim 20$ kpc do we note some patches of lower star formation [Fe/H]. We note that Buck et al. (2023) found considerable dips in the gas metallicity [Fe/H] of this simulation during the merger. By comparison with the positions of the major merger galaxy around this time (see Fig. 9b from Paper I), we can confirm those as accreted structures as well. This again underlines our impression of no significant lowering of star formation [Fe/H] during the merger. For all remaining epochs, we only notice a rather uneventful inside-out star formation with a radial metallicity gradient (see also Buder et al. 2025a).

4 DISCUSSION

In Paper I, we examined the efficiency of recovering accreted stars in integral-of-motion space and assessed how much information about their birth positions and chemistry is preserved. Here, we extend this framework to focus on what can be inferred from birth positions, ages, and chemistry about the dynamical state of the early disc, and in particular on the proposed splashing of the Milky Way's protodisc (Belokurov et al. 2020).

4.1 The nature of Splash-like stars

Our analysis of Splash-like stars in a Solar-like neighbourhood with low azimuthal velocities and subsolar metallicities (Figs. 1–6) suggests that these stars represent the ancient portion of the protodisc, in line with earlier observational studies (Bonaca et al. 2017; Haywood et al. 2018; Di Matteo et al. 2019; Gallart et al. 2019; Belokurov et al. 2020). Similar to Belokurov et al. (2020), we find that the properties of these stars bridge smoothly to those of the thick disc. However, when comparing stars with similar chemistry and ages, we also identify prograde counterparts with high V_φ, and that the V_φ distribution of the sample shows a positive skewness (Fig. 4). This indicates that the majority of stars in this population already occupy lower V_φ orbits, rather than being drawn from a dynamically cold distribution that was later heated. The latter would lead to a negative skewness with a higher mean V_φ, which is inconsistent with our findings.

This challenges the interpretation that the Splash is simply the tail of a cold protodisc violently heated by *GSE* (Di Matteo et al. 2019; Belokurov et al. 2020). Instead, our findings align more closely with the results of Amarante et al. (2020), who showed in an isolated clumpy disc simulation that stars can be *born hot* on halo-like orbits while retaining thick-disc chemistry. Our analysis of birth positions strengthens this view: we find no significant radial or vertical displacement between average present-day and birth positions ($\overline{\Delta R_{\rm 2D}} = \overline{R_{\rm 2D,birth} - R_{\rm 2D}} = -0.1^{+1.1}_{-1.2}$ kpc, $\overline{\Delta|Z|} = \overline{|Z_{\rm birth}| - |Z|} = 0.03^{+0.70}_{-0.68}$ kpc), questioning the need for a large-scale dynamical splashing event.

4.2 Implications for disc heating and angular momentum build-up

The galaxy in which Splash stars formed was not yet rotation-dominated. In the simulation, a rotation-supported disc emerges only ~ 9.5 Gyr ago, consistent with observational inferences of a gradual increase in disc rotation from 11 to 8 Gyr ago (e.g. Minchev et al. 2013). Whether this angular momentum build-up was causally linked to the last major merger remains uncertain. While some studies argue that *GSE* heating produced the Splash (Bonaca et al. 2020; Di Matteo et al. 2019), our results suggest that at least part of the population was already dynamically hot. The reality may well involve a combination of both effects, as also hinted by cosmological simulations that show Splash-like stars arising in multiple pathways, including major mergers, retrograde minor mergers, and secular processes (Quinn et al. 1993; Purcell et al. 2010; Villalobos & Helmi 2008, 2009; Dillamore et al. 2023; Dillamore & Sanders 2025; Kisku et al. 2025). While secular processes such as bar resonances have also been shown as a possible pathway to generate Splash-like signatures (Dillamore et al. 2022, 2023), we note that the NIHAO-UHD simulation analysed here does not form a significant present-day bar (Buder et al. 2025a). This makes it unlikely that bar-driven resonances are responsible for the Splash-like stars we identify at $z = 0$, at least in this particular simulation.

Quantifying the merger contribution to angular momentum evolution is a broader challenge. The outcome depends on mass ratios, orbital configurations, and the timing of gas inflows (e.g. Lagos et al. 2017, 2018). A single simulation cannot establish causality, but suites of cosmological simulations offer promising routes forward (Pillepich et al. 2019; Sotillo-Ramos et al. 2022). Our findings underscore the need for such systematic studies to disentangle the relative importance of heating versus hot-born origins.

4.3 Limitations and outlook

In this work our analysis focused solely on the stellar component, in line with current observations. We do not explicitly follow gas inflows onto the Milky Way analogue or the gas content of the major merger, which are known to influence the degree of mixing and subsequent star formation (e.g. Cooper et al. 2015; Agertz et al. 2021; Renaud et al. 2021; Buck et al. 2023). Future work combining stellar and gaseous tracers may better constrain the role of gas-rich accretion in producing stars with Splash-like properties.

As more precise observational constraints become available, particularly in ages and multi-element abundance patterns, it should become possible to further test whether Splash-like stars were primarily heated, born hot, or both. The emerging diversity of predictions across simulation suites (Brooks et al. 2025) highlights the value of confronting these with observationally defined populations. Our results demonstrate that cosmological simulations with traced birth positions provide a crucial tool for this task, moving beyond kinematics alone and towards a more nuanced understanding of the Splash as a window into the Milky Way's early disc and merger history.

5 CONCLUSIONS

In Paper I, we established the framework for interpreting the last major merger of a Milky Way analogue, focusing on selection efficiency and the retention of chemodynamical memory. Here, we have used the same NIHAO-UHD simulation to examine the proposed

Splash population, enabled by tracing the birth positions, ages, and chemistry of stars.

Our analysis finds no significant evidence for a large-scale dynamical splashing of in-situ stars. Instead, protodisc stars – including those with present-day low azimuthal velocities – were already born on dynamically hot orbits in a turbulent early disc. The transition to a rotation-supported disc occurs only during or after the merger. This suggests that much of the observed Splash may not require violent heating by the *GSE* merger, but can arise naturally from stars formed in a thick, kinematically hot disc, later intermixed with accreted stars and stars formed from merger-driven gas inflows.

These results place our simulation in closer agreement with models in which Splash-like populations are *born hot* (e.g. Amarante et al. 2020) during the spin-up phase (e.g. Yu et al. 2023a), while still acknowledging that merger-induced heating may contribute, as argued by other studies (e.g. Di Matteo et al. 2019; Belokurov et al. 2020; Bonaca et al. 2020). Together with recent evidence from cosmological simulations and observations (Dillamore et al. 2022, 2023; Khoperskov et al. 2023b; Dillamore & Sanders 2025; Kisku et al. 2025), this highlights that Splash-like stars likely arise through a combination of pathways rather than a single mechanism.

We conclude that the interpretation of the Splash as a distinct, merger-heated population is overly restrictive. A more nuanced view is required, in which kinematics, chemistry, and formation history jointly contribute to the observed distribution of stars. Cosmological simulations with birth-position information provide a critical benchmark for disentangling these processes, and future simulation suites will be essential for quantifying the balance between heated and born-hot origins in the context of the Milky Way's early assembly.

ACKNOWLEDGMENTS

We acknowledge the traditional owners of the land on which the ANU stands, the Ngunnawal and Ngambri people. We pay our respects to elders past, and present and are proud to continue their tradition of surveying the night sky and its mysteries to better understand our Universe. SB acknowledges support from the Australian Research Council under grant number DE240100150. TB's contribution to this project was made possible by funding from the Carl Zeiss Stiftung. ÁS acknowledges funding from the European Research Council (ERC) under the European Union's Horizon 2020 research and innovation programme (grant agreement No. 101117455).

DATA AVAILABILITY

All code to reproduce the analysis and figures can be publicly accessed via `https://github.com/svenbuder/golden_thread_II`. The used simulation snapshot can be publicly accessed as FITS file via `https://github.com/svenbuder/preparing_NIHAO`. Original data, more snapshots and other galaxies can be found at `https://tobias-buck.de/#sim_data`. We encourage interested readers to get in contact with the authors for full data access and advice for use and cite Buck et al. (2020, 2021).

SOFTWARE

The research for this publication was coded in PYTHON (version 3.12.11) and included its packages ASTROPY (v. 7.1.0; Astropy Collaboration et al. 2013, 2018), HYPPO (v. 0.5.2; Panda et al. 2019), IPYTHON (v. 9.1.0; Pérez & Granger 2007), MATPLOTLIB (v. 3.10.3; Hunter 2007), NUMPY (v. 2.2.6; Walt et al. 2011), as well as SCIPY (v. 1.16.0; Virtanen et al. 2020). We used TOPCAT (v. 4.7; Taylor 2005).

REFERENCES

Agertz O., et al., 2021, MNRAS, 503, 5826
Amarante J. A. S., Beraldo e Silva L., Debattista V. P., Smith M. C., 2020, ApJ, 891, L30
Amarante J. A. S., Debattista V. P., Beraldo e Silva L., Laporte C. F. P., Deg N., 2022, ApJ, 937, 12
Astropy Collaboration et al., 2013, A&A, 558, A33
Astropy Collaboration et al., 2018, AJ, 156, 123
Belokurov V., Kravtsov A., 2022, MNRAS, 514, 689
Belokurov V., Erkal D., Evans N. W., Koposov S. E., Deason A. J., 2018, MNRAS, 478, 611
Belokurov V., Sanders J. L., Fattahi A., Smith M. C., Deason A. J., Evans N. W., Grand R. J. J., 2020, MNRAS, 494, 3880
Bonaca A., Conroy C., Wetzel A., Hopkins P. F., Kereš D., 2017, ApJ, 845, 101
Bonaca A., et al., 2020, ApJ, 897, L18
Brooks R. A. N., Sanders J. L., Dillamore A. M., Garavito-Camargo N., Price-Whelan A. M., 2025, arXiv e-prints, p. arXiv:2507.10667
Brown A. G. A., 2021, ARA&A, 59, 59
Buck T., 2020, MNRAS, 491, 5435
Buck T., Macciò A. V., Dutton A. A., Obreja A., Frings J., 2019, MNRAS, 483, 1314
Buck T., Obreja A., Macciò A. V., Minchev I., Dutton A. A., Ostriker J. P., 2020, MNRAS, 491, 3461
Buck T., Rybizki J., Buder S., Obreja A., Macciò A. V., Pfrommer C., Steinmetz M., Ness M., 2021, MNRAS, 508, 3365
Buck T., Obreja A., Ratcliffe B., Lu Y., Minchev I., Macciò A. V., 2023, MNRAS, 523, 1565
Buder S., et al., 2022, MNRAS, 510, 2407
Buder S., Mijnarends L., Buck T., 2024, MNRAS, 532, 1010
Buder S., Buck T., Chen Q.-H., Grasha K., 2025a, OJAp, 8, 47
Buder S., Buck T., Skúladóttir A., Ness M., McKenzie M., Monty S., 2025b, arXiv e-prints, arXiv:2510.11284, Paper I
Carrillo A., Deason A. J., Fattahi A., Grand R. J. J., Fragkoudi F., 2025, arXiv e-prints, p. arXiv:2509.24705
Chandra V., et al., 2024, ApJ, 972, 112
Cooper A. P., Parry O. H., Lowing B., Cole S., Frenk C., 2015, MNRAS, 454, 3185
Di Matteo P., Haywood M., Lehnert M. D., Katz D., Khoperskov S., Snaith O. N., Gómez A., Robichon N., 2019, A&A, 632, A4
Di Matteo P., Spite M., Haywood M., Bonifacio P., Gómez A., Spite F., Caffau E., 2020, A&A, 636, A115
Dillamore A. M., Sanders J. L., 2025, MNRAS, 542, 1331
Dillamore A. M., Belokurov V., Font A. S., McCarthy I. G., 2022, MNRAS, 513, 1867
Dillamore A. M., Belokurov V., Evans N. W., Davies E. Y., 2023, MNRAS, 524, 3596
Font A. S., et al., 2020, MNRAS, 498, 1765
Frankel N., Rix H.-W., Ting Y.-S., Ness M., Hogg D. W., 2018, ApJ, 865, 96
Frankel N., Sanders J., Ting Y.-S., Rix H.-W., 2020, ApJ, 896, 15
Gallart C., Bernard E. J., Brook C. B., Ruiz-Lara T., Cassisi S., Hill V., Monelli M., 2019, Nature Astronomy, 3, 932
Gretton A., Borgwardt K. M., Rasch M. J., Schölkopf B., Smola A., 2012, Journal of Machine Learning Research, 13, 723
Haywood M., Di Matteo P., Lehnert M. D., Snaith O., Khoperskov S., Gómez A., 2018, ApJ, 863, 113
Helmi A., 2020, ARA&A, 58, 205
Helmi A., Babusiaux C., Koppelman H. H., Massari D., Veljanoski J., Brown A. G. A., 2018, Nature, 563, 85
Hodges J. L., 1958, Arkiv for Matematik, 3, 469
Hunter J. D., 2007, Comput Sci Eng, 9, 90
Jofré P., Heiter U., Soubiran C., 2019, ARA&A, 57, 571

Khoperskov S., Minchev I., Steinmetz M., Marabotto J., Kordopatis G., Delgado Gomez J., Libeskind N., 2023a, arXiv e-prints, p. arXiv:2310.05287
Khoperskov S., et al., 2023b, A&A, 677, A89
Kisku S., et al., 2025, MNRAS, 542, 76
Lagos C. d. P., Theuns T., Stevens A. R. H., Cortese L., Padilla N. D., Davis T. A., Contreras S., Croton D., 2017, MNRAS, 464, 3850
Lagos C. d. P., et al., 2018, MNRAS, 473, 4956
Minchev I., Chiappini C., Martig M., 2013, A&A, 558, A9
Mori A., Di Matteo P., Salvadori S., Khoperskov S., Pagnini G., Haywood M., 2024, A&A, 690, A136
Naidu R. P., Conroy C., Bonaca A., Johnson B. D., Ting Y.-S., Caldwell N., Zaritsky D., Cargile P. A., 2020, ApJ, 901, 48
Naidu R. P., et al., 2021, ApJ, 923, 92
Panda S., Palaniappan S., Xiong J., Bridgeford E. W., Mehta R., Shen C., Vogelstein J. T., 2019, arXiv e-prints, p. arXiv:1907.02088
Pérez F., Granger B. E., 2007, Comput Sci Eng, 9, 21
Pillepich A., et al., 2019, MNRAS, 490, 3196
Planck Collaboration et al., 2014, A&A, 571, A16
Purcell C. W., Bullock J. S., Kazantzidis S., 2010, MNRAS, 404, 1711
Quinn P. J., Hernquist L., Fullagar D. P., 1993, ApJ, 403, 74
Renaud F., Agertz O., Andersson E. P., Read J. I., Ryde N., Bensby T., Rey M. P., Feuillet D. K., 2021, MNRAS, 503, 5868
Sotillo-Ramos D., et al., 2022, MNRAS, 516, 5404
Stinson G., Seth A., Katz N., Wadsley J., Governato F., Quinn T., 2006, MNRAS, 373, 1074
Stinson G. S., Brook C., Macciò A. V., Wadsley J., Quinn T. R., Couchman H. M. P., 2013, MNRAS, 428, 129
Taylor M. B., 2005, ASPC, 347, 29
Vasiliev E., 2019, MNRAS, 482, 1525
Villalobos Á., Helmi A., 2008, MNRAS, 391, 1806
Villalobos Á., Helmi A., 2009, MNRAS, 399, 166
Virtanen P., et al., 2020, Nature Methods, 17, 261
Wadsley J. W., Keller B. W., Quinn T. R., 2017, MNRAS, 471, 2357
Walt S. v. d., Colbert S. C., Varoquaux G., 2011, Comput Sci Eng, 13, 22
Wang L., Dutton A. A., Stinson G. S., Macciò A. V., Penzo C., Kang X., Keller B. W., Wadsley J., 2015, MNRAS, 454, 83
Yu J., Khanna S., Themessl N., Hekker S., Dréau G., Gizon L., Bi S., 2023a, ApJS, 264, 41
Yu S., et al., 2023b, MNRAS, 523, 6220